IEEE Access
Multidisciplinary ⋮ Rapid Review ⋮ Open Access Journal

Received 25 July 2024, accepted 9 August 2024, date of publication 13 August 2024, date of current version 3 September 2024.

Digital Object Identifier 10.1109/ACCESS.2024.3443138

RESEARCH ARTICLE

IoT-Based IGBT Power Module Health Monitoring System With RUL Estimation for Electric Drive Applications

R. MANIKANDAN[1] AND R. RAJA SINGH[2], (Member, IEEE)
[1]School of Electrical and Electronics Engineering, Vellore Institute of Technology, Vellore, Tamil Nadu 632014, India
[2]Automotive Research Center, Vellore Institute of Technology, Vellore, Tamil Nadu 632014, India

Corresponding author: R. Raja Singh (rrajasingh@gmail.com)

ABSTRACT Insulated Gate Bipolar Transistor (IGBT) is a crucial and sensitive component in electric motor drive applications, and its reliability has gained significant research attention. Estimating the remaining life of converter IGBTs is essential for enhancing the safety and dependability of these applications while minimizing maintenance costs. Most of the existing work in the literature concentrated on accelerated age testing on a single IGBT switch or module. However, in a practical environment, various operational parameters affect the life of IGBT-based converters. This paper proposes a novel framework to estimate the IGBT power module's remaining useful lifetime (RUL) and enable failure prediction. This method can also be employed as a converter design method or an online lifetime estimation scheme when applied to real systems. To validate the developed technique, it is applied to a direct torque-controlled induction motor drive in the PLECS hardware-in-loop system. The load/mission profile is generated with a 3.7 kW induction motor driven by a three-phase 2-level voltage source inverter (3-phase 2L VSI). The temperature of the IGBT is estimated based on a time-dependent temperature calculation, and hence the depreciation of the IGBT power device is anticipated. The outcome of the research reveals realistic information on significant influences on the 3-phase 2L VSI's lifetime under various operational range characteristics. The outcome of the research reveals realistic information about the key factors that affect the 3-phase 2L VSI's lifetime during changes in operational conditions. From the RUL results, the load current and switching frequency variations influence the remaining life of the power devices in the electric drive system. Finally, a Matlab GUI application is created to estimate the inverter's lifetime, based on junction temperature data from a specific mission profile. The proposed system also incorporates the IoT real-time temperature monitoring of the IGBT power module and heat sink under various operating conditions IM drive.

INDEX TERMS Rainflow, lifetime, motor drive, half-bridge power modules, real-time mission profile, IoT, temperature monitoring.

I. INTRODUCTION

The prognosis and health management (PHM) of electric machine drives are crucial due to their extensive applications in industry and transportation. Advanced sensors, communication, computing technology, and theories offer increasingly effective resources for implementing dependable PHM solutions. Robust systematic predictions and health monitoring serve as the essential foundation for numerous commercial systems of engineering [1]. It may be possible to increase the reliability of the power converter and machines by replacing worn-out parts before they fail. Compared to machines, power converters are much more vulnerable and hence it is important to assess the lifetime of the IGBT power modules in electric drive systems. The electric drive system includes AC to DC converter, DC link capacitors, DC to AC inverters, sensors, and auxiliary circuits. Among these, the DC to AC inverter causes 38% of drive failures, hence it is an important

The associate editor coordinating the review of this manuscript and approving it for publication was Nagesh Prabhu.

© 2024 The Authors. This work is licensed under a Creative Commons Attribution-NonCommercial-NoDerivatives 4.0 License.
For more information, see https://creativecommons.org/licenses/by-nc-nd/4.0/

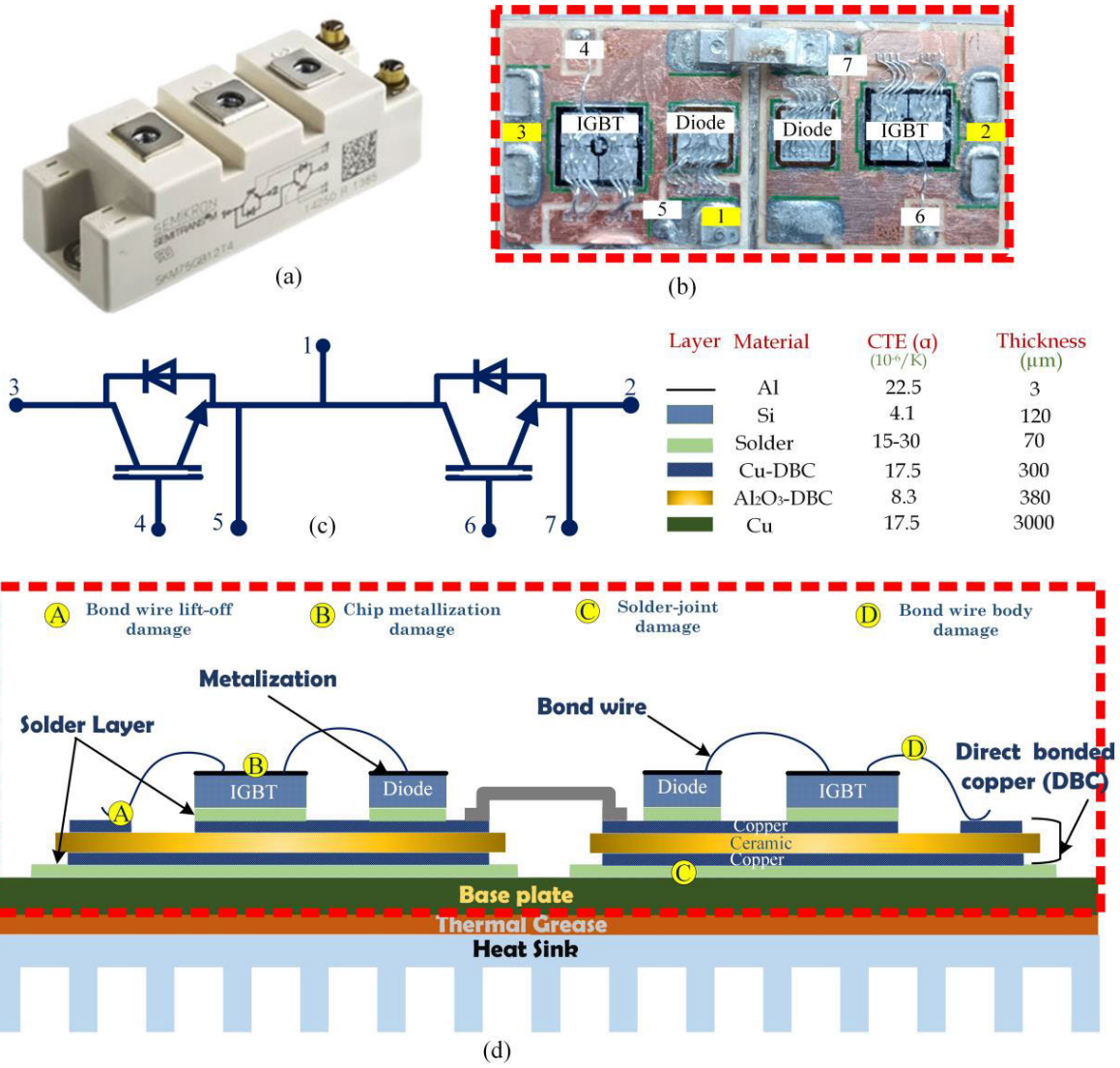

FIGURE 1. The power module detailed internal structure and schematic diagram; (a) SEMIKRON (SKM100GB12T4) power module, (b) Internal view of SKM100GB12T4, (c) Circuit diagram of IGBT half-bridge, (d) Cross sectional schematic of half-bridge power module.

component to monitor [2]. The inverter failure is attributed to IGBT devices, which account for approximately 31% of the overall converter failure issues [3]. The IGBT Power modules used in motor drives are exposed to extreme conditions and operate in challenging environments. Thermal stresses resulting from the mean temperatures and temperature fluctuations are the primary reasons for power device ageing failure. The multi-chip parallel technology employed in IGBT power modules, whether pressed or welded, satisfies the demands for high voltage and high current. Nevertheless, it brings about the issue of uneven temperature distribution [4], [5] Hence, ensuring the dependability and longevity of such devices is highly significant.

A. STATE OF THE ART TECHNIQUES

Fig. 1 illustrates the detailed internal structure of the IGBT-based power module and schematic diagram. Fig. 1(a) shows the SEMIKRON (SKM100GB12T4) power module, and Fig.1(b) depicts the internal chip arrangement and bond wire connections of the half-bridge power module, which shows the two IGBT chips and two antiparallel diode chips. Fig. 1c shows the connection between different parts shown in Fig. 1(b). The IGBT module is made up of several components, including the heat sink, base plate, direct bond copper substrate (DBC), and chip, as shown in Fig. 1(d) [6]. Failures in IGBT devices are categorized into two types; failure due to package, and failure due to chips. Also, catastrophic failure is caused due to over-voltage, over-current, or electrical overstress during operation. Research on reliability for silicon-based IGBT modules currently emphasizes package-related failures [7]. The periodic application of thermal and electrical stress, as well as the wire's bending stress, form a fracture in between the aluminium lead and silicon chip that progressively increases. This ultimately causes bond wire lift-off and fatigue in the solder layer [8]. The primary reason for IGBT power module age-related failure is caused

due to internal temperature variation and mismatched CTE (thermal expansion coefficient) among various layers. This results in cyclic thermal and electrical stress. Studies indicate that wire-bond failure is associated with fast power cycling (spanning 10s) and greater temperature variation ($\Delta T >$ 100 K), whereas, solder fatigue-related failures are linked to slow power cycling (taking more than 10 min.) and lesser temperature variation ($\Delta T <$ 80 K) [9]. The IGBT modules in the converter commonly experience bond wire fatigue, aluminium reconstruction, solder fatigue, and gate oxide degradation as their failure [10].

The fault diagnosis is primarily used to determine the cause of the IGBT module's abnormal health state. To enhance the power module reliability, researchers are focused on fault diagnosis, condition monitoring, active thermal control, and life prediction. Accurately estimating the health condition and RUL of IGBT is crucial for effectively transferring mechanical systems through power converters. In general, the lifetime of power components can be estimated by considering model-driven and data-driven approaches. The model-driven approach can be either empirical [11], [12] or physics-based [13]. Models integrating with Miner's rule [14] allow estimating the lifetime by considering a given mission profile in terms of temperature swing, average temperature, heating time, and current density [15]. The data-driven approach is based on the monitoring of the State of Health (SoH) of the component. In the case of wire bond degradation, on-voltage is usually adopted as a precursor, while in the case of solder joint fatigue, the thermal impedance gives a better indication of the SoH [16]. The knowledge of the SoH allows for implementing prognostic techniques and hence estimating the RUL. The implementation of prognostic techniques is the key to achieving predictive maintenance and hence to avoid catastrophic failure events [17], [18], [19].

In power modules, mainly the bond wire lift-off occurs owing to fracture within the wire bond. To address this problem, in [18] the FE (finite element) analysis is used to develop a correlation between the growth of every bond wire's fracture length and variation in V_{CE}, which enables an effective prediction of RUL. Normally, the lifetime of a high-power IGBT module is determined by the thermal cycles as a function of stress parameters. This model is developed based on experimental data from accelerated power-cycling tests performed at predefined temperature stress conditions. In [20], proposes a deep learning-based model for predicting the lifetime of power devices subjected to power cycling. To this purpose, a neural network based on bidirectional long short-term memory is adopted. The neural network is trained with experimental on-voltage degradation processes. The application of the proposed method is based on the monitoring of a precursor which is the on-voltage degradation. According to the considered precursor, the model allows predicting the RUL of power components. In [21], the RUL of high-power IGBT modules is estimated subjecting them to power cycling tests involving low-temperature stress cycles at 30° C and 40° C. The traditional thermal tress cycle counting algorithms do not consider the time-dependent mean temperature. In [22], the lifespan of passively cooled power modules in a tidal turbine converter is studied under the effect of waves travelling across the surface and turbulence in tidal current speed. One of the recent works addressed the effect of the likelihood of failure for power devices (SiC) in the reliability of battery-operated EVs in the automotive field [23]. However, the major drawback of this method fails to consider the real-time junction temperature for the lifetime estimation model. Previous studies of lifetime prediction focus mainly on the device level, but this paper proposes an improved methodology for real-time estimation of inverter lifespan in motor drive systems, considering various operating conditions and load profiles.

B. CONTRIBUTION OF THE PAPER

The proposed approach combines electro-thermal simulation using device models with thermal stress-based damage assessment with an accurate thermal profile. With proper calibration of the system model, this method can estimate the inverter lifespan for any mission profile accurately. Specifically focused on predicting the lifetime of 2L voltage source inverters used in electric motor drives.

This article's contributions are listed as follows:

- Accurate thermal modelling of the inverter through iterative, real-time data.
- Along with the load cycles and specific operating conditions, the dynamic environmental conditions were also considered.
- The RUL of the inverter is estimated with the variation of switching frequency, speed, and torque of the drive system.
- Developing a Matlab GUI-based application to estimate the inverter's lifetime based on temperature profiles provided.
- IoT-based real-time IGBT modules junction temperature monitoring with email notification for critical decision making.

The remaining article is structured as follows. Section II discusses the development of a power loss-based IGBT junction temperature estimation model. The proposed methodology with details of the remaining lifetime estimation process is explained in section III. The real-time experimental setup and power cycling data collection are detailed in section IV. Section V presents the RUL estimation simulation and experimental results. The Matlab App implementation and IoT integration to the proposed work are discussed in section VI, and the article is concluded in section V.

II. POWER LOSS BASED JUNCTION TEMPERATURE ESTIMATION MODEL

Various methods like finite element (FE) and finite difference (FD) techniques are recognized for their ability to accurately conduct thermal analysis of intricate geometries, enabling the attainment of the device's internal temperature

[24]. However, they are computationally intensive and require more time frames to estimate the internal temperatures of power devices. To address this issue, the thermal network of IGBT devices is effective in terms of time and can be rapidly incorporated into different circuit simulators including PLECS [25]. Thermal equivalent circuits (TECs) are classified into the foster chain and Cauer ladder, it is due to their thermal resistance (Rth) and capacitance (Cth). The Cauer model relies on the IGBT device's physical data, while the Foster model is fitted mathematically using experimental data. Foster-type TECs have no filtering effect on injected power loss, leading to errors in transient temperatures under fast-varying loads. In contrast, Cauer-type TECs over-filter power loss causing larger errors in steady-state temperatures. Due to its reflection of 3-D heat dissipation in the layers of a material, the more accurate and popular choice among researchers and designers is the foster model. This article establishes a foster-type model utilizing electro-thermal simulations.

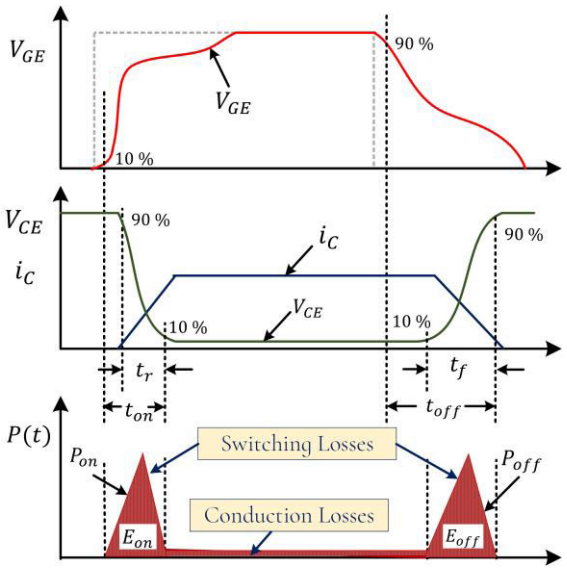

FIGURE 2. Transient switching process and Loss profile of IGBT.

A. POWER LOSS CALCULATION

Considering heat flow as power loss in a traditional RC network thermal model can predict the junction temperature quickly. However, the relation between thermal and electrical parameters is not linear, this technique is restricted to accurate loss computation [26]. The calculation of power loss in 3-phase 2L-VSI primarily pertains to IGBTs and anti-parallel diodes. Typically, in power semiconductor-based converter systems, the switching and conduction losses are the major components denoted by (1).

$$P_{tot(IGBT)} = P_{ON} + P_{OFF} + P_{con\_IGBT} \tag{1}$$

Fig. 2 displays the switching characteristics of IGBT and its loss profile. As expressed in (1) the total power loss of IGBT ($P_{tot(IGBT)}$) is composed of on-state power dissipation (P_{con_IGBT}), turn–on loss (P_{ON}) and turn-off loss (P_{con_IGBT}).Similarly, in the case of a freewheeling diode the total power dissipation ($P_{tot(D)}$) is contributed by turn-on power loss (P_{con_D}) and the reverse recovery of the power diode (P_{rec}).

$$P_{tot(D)} = P_{con\_D} + P_{rec} \tag{2}$$

B. THERMAL EQUIVALENT CIRCUIT OF IGBT SWITCH

The thermal modelling methods for IGBT modules are focused in this section. The estimation of T_j is done using streamlined TEC models. In Fig. 3, the RC components are utilized to depict thermal impedances between different components. The base plate, IGBT devices, and reverse diodes in the power modules are thermally coupled, and their temperatures can be assumed to be the same for simplification purposes. In the power module, the total energy losses of all internal elements have to be absorbed in the thermal impedance $Z_{th(c-s)}$ (Fig.3a). As previously discussed, TECs are derived from designing the thermal impedance in the form of chain-type "mathematical" TECs (Fig. 3b, "Foster network") and ladder-type "physical" TECs (Fig.3c, "Cauer network"). By analyzing the temperature variations of T_j, T_c, T_s, and T_a over time, the $Z_{th(j-c)}$, $Z_{th(c-s)}$, and $Z_{th(s-s)}$ for thermal impedances are estimated. These are represented as four poles in TECs using measures of geometry and material characteristics. At least one RC model is needed for each layer in the structure, with subsequent adjustments often necessary to match measured results. A chain-type (Foster) equivalent circuit diagram can be obtained by determining factors and time constants through formula manipulation.

$$Z_{th(x-y)} = R_{th1}\left(1 - e^{\frac{-t}{\tau_{th1}}}\right) + R_{th2}\left(1 - e^{\frac{-t}{\tau_{th2}}}\right) + R_{th3}\left(1 - e^{\frac{-t}{\tau_{th3}}}\right) + \ldots \tag{3}$$

where two to three exponential terms are enough for the representation of TECs. The exponential function's primary benefit is its suitability for calculating subsequent temperatures. SEMIKRON IGBT modules specify parameters for $Z_{th(j-c)} \backslash Z_{th(j-s)}$ in 2 to 6 RC components in their application notes [27], enabling CAD simulations of junction temperature. The equivalent circuits of both sub-blocks may be aligned within the general system, allowing for the determination of intermediate temperatures T_c and T_s. By manipulating formulas, one can obtain a foster-equivalent circuit diagram based on factors and time constants.

The thermal equivalent circuits are essential for the accurate estimation of the junction temperature of the IGBT in the power module. Further, these network data are utilized to collect thermal stress information of power modules during various mission profiles of the inverter. Finally, the thermal stress information from TECs acts as the major component to estimate the remaining useful lifetime of power modules for different operating conditions of the motor drive. The

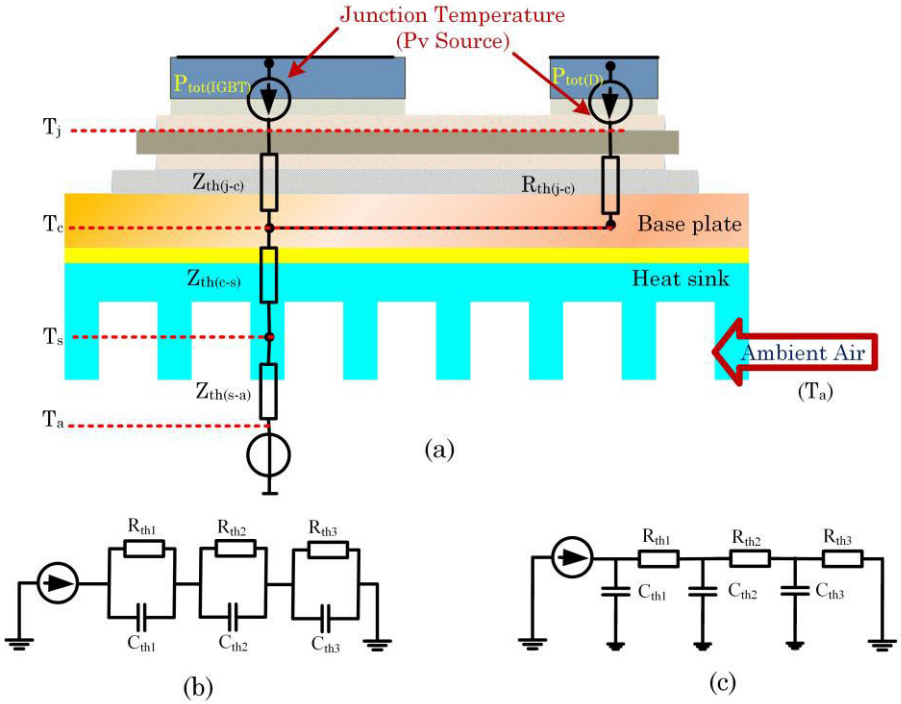

FIGURE 3. Thermal model of IGBT with antiparallel diode; (a) representation IGBT module by means of thermal impedance network (N/W), (b) chain-class "mathematical" equivalent circuit (Foster N/W), (c) conductor-class "physical" equivalent circuit (Cauer N/W).

following section details the proposed framework for RUL estimation power modules in electric drive applications.

III. PROPOSED FRAMEWORK FOR SYSTEM LEVEL RUL ESTIMATION

To assess the remaining useful time of the 3-phase 2L-VSI in motor drive applications, it is necessary to follow the comprehensive progressive procedure illustrated in Fig. 4. This involves translating mission profiles into thermal stress functions and then converting them to an estimation of damage accumulation.

A. ACCURATE THERMAL STRESS PROFILE COLLECTION

The proposed framework for lifetime estimation of 3-phase 2L-VSI considers the motor speed and load torque, dc-link voltage and switching frequency as an inverter mission profile. Power and energy losses from IGBT power modules are estimated using mathematical calculations (1)-(3). It provides an easy approximation of average power losses during switching periods. This data is used to determine thermal stress on components during operation via thermal models. In the proposed methodology an iterative experimental data-based accurate thermal modelling of the inverter is achieved, which helps to estimate the remaining useful lifetime of the inverter. The power loss look-up tables (LUTs) are formed by simulating power devices for various operating conditions and forward IV characteristics. LUTs for conduction power dissipation can be built using the forward IV characteristics of the device. The manufacturer data sheet and real-time experiments were used to determine both switching and conduction losses for IGBT and diode, as illustrated in Fig. 5. The thermal networks are extracted from the PLECS software environment to further modify the electro-thermal model. The extracted thermal impedance network undergoes modification to minimize the difference between simulation outputs and real-time experiment outputs. Once configured, the electro-thermal simulation accurately reflects the inverter's behaviour by using validated power loss LUTs and thermal networks from experimental data. Fig. 5 illustrates the closed loop direct torque controlled (DTC) 3-phase 2L-VSI fed induction motor which is modelled in the PLECS software environment. The IGBT power module's junction temperature changes according to mission profile variation, which can cause fatigue failure in power electronics components. To assess this, the temperature stress cycles (N_i) need to be counted, furthermore, temperature variation (ΔT_j), pulse period of IGBTs (t_{ON}), and average junction temperature (T_{jm}) also have to be calculated. This can be achieved with the help of the rainflow counting algorithm, which is the popular counting algorithm recommended by ASTM (formerly known as the American Society for Testing and Materials). This algorithm converts the irregular thermal cycles from various mission profiles into regular thermal stress cycles.

B. ASSESSMENT OF REMAINING USEFUL LIFETIME

As discussed in section II, accurate electro-thermal models are utilized for the estimation of junction temperature during

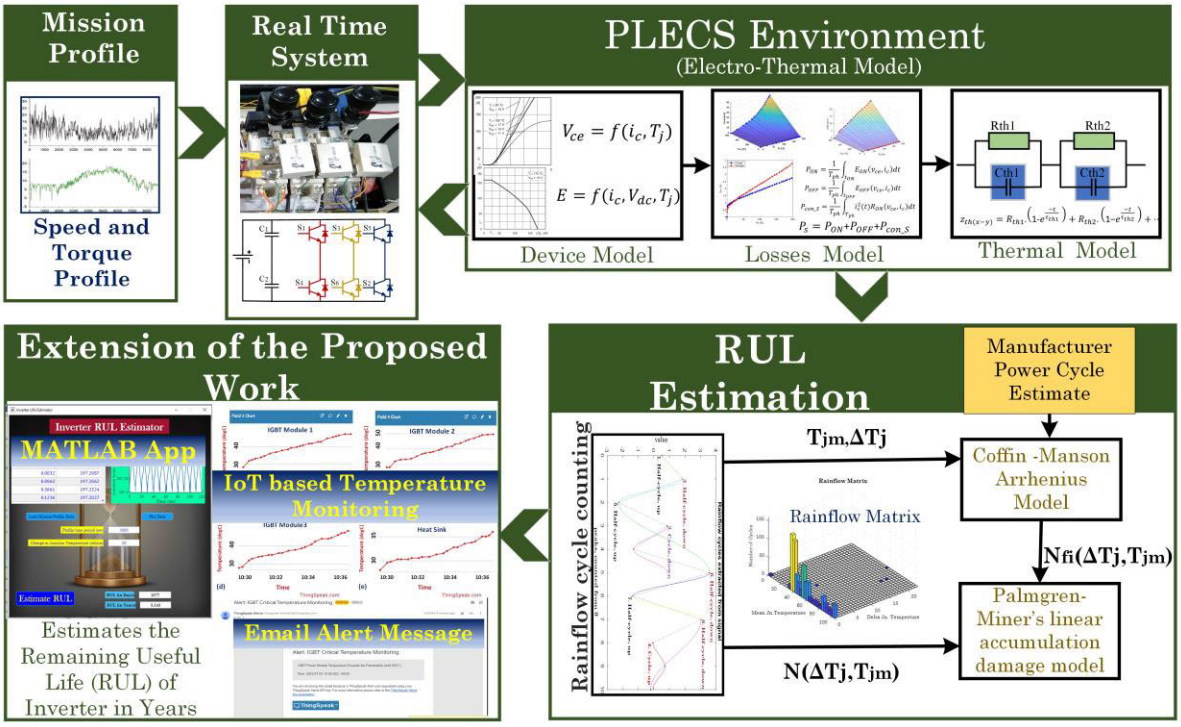

FIGURE 4. Detailed scheme of proposed RUL assessment of the 2L-VSI for the Motor drive platform.

various mission profiles of IM drive. To estimate the power transistor's RUL during real-time operating conditions, the conventional rainflow cycle counting technique is used to putrefy temperature stress profiles into cycles with amplitude, and based on the outcome cycle counting algorithm accumulated damage is calculated.

1) RAINFLOW ALGORITHM BASED CYCLE COUNTING METHOD

Various additional cycle counting techniques are being developed, such as level crossing, peak counting, and basic range/mean counting. Nevertheless, they fall short of capturing all the attributes required for an accurate fatigue failure investigation. The rainflow cycle counting method created by Endo and Matsuishi (pagoda roof algorithm) overcomes this limitation [28], [29], which is the popular cycle counting technique used in a fatigue failure investigation. The physical meaning of the rainflow counting technique to counting the temperature cycle is based on the hysteresis loop. The Rainflow algorithm requires only the extreme points; as a result, more stress load profile points must be eliminated. Additionally, since smaller stress cycles have minimal impact on lifetime, their impact must also be disregarded.

Rainflow algorithm working process;

i) Initially, the temperature cycle history and time axis will be oriented vertically, with increasing time downward.
ii) Rearrange cycle data to begin and end at the value of greatest amplitude.
iii) Cycles are defined in which rain is allowed to "drip" or "fall"
iv) Every time there has been a reversal in the flow of rain, it is allowed to continue unless

- It encounters a previous rainflow
- The rain started at a local maximum (or minimum) point and fell in the opposite direction from where it originated.

According to the rainflow algorithm for Fig. 6(a)), Table 1 shows the steps involved.

Bond wire lift-off and solder fatigue are two dominant degradation mechanisms in multi-chip power modules. These failures are primarily caused by thermal cycling (fluctuations) developed in the multi-layered package and are associated with variable thermal expansion coefficients (CTE) for the components. In this article, the damage refers to the cumulative damage that occurs to the power module due to temperature fluctuations in the inverter due to various mission profiles.

2) DAMAGE ACCUMULATION METHOD

The Arrhenius-Coffin-Manson's lifetime model is an equation that was introduced by Held et.al in 1964 [30]. It explains the connection between a material's life in terms of cycles, its average temperature, and the temperature range. Here the improved lifetime estimation model has been

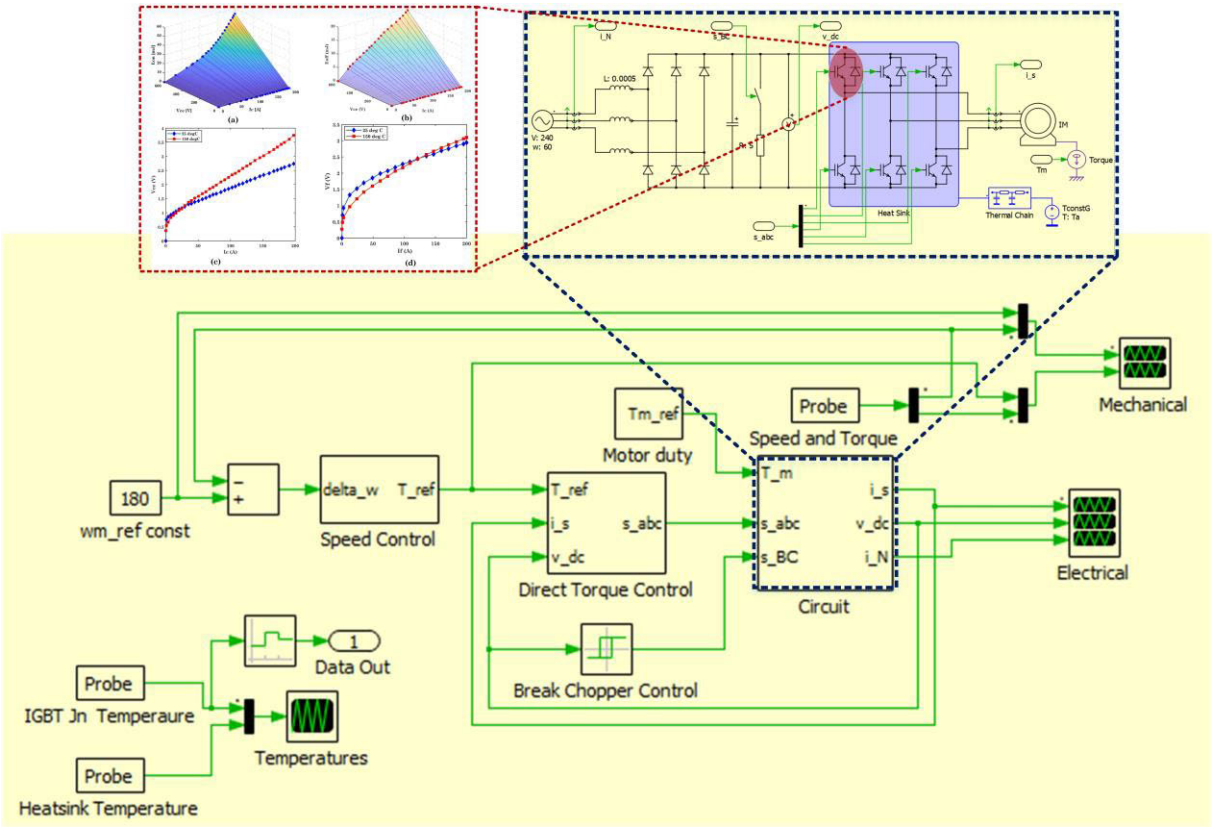

FIGURE 5. DTC based closed control induction motor drive realized in PLECS environment.

incorporated [28] as shown in (4)

$$N_f = A_0 \times A_1^{\beta} \times \Delta T_j^{-\beta_1} \times \Delta T_j^{\alpha} \times exp\left(\frac{E_a}{k_B.T_{jm}}\right) \times \frac{C + t_{on}^{\gamma}}{C + 2^{\gamma}} \times k_{thickness} \quad (4)$$

With $\beta = e^{\left(\frac{-(\Delta T_j - T_0)}{\lambda}\right)}$

Here, N_f represents the number of cycles until failure, ΔT_j is the temperature change, Tjm is the average temperature of the IGBT junction, E_a activation energy, $k_{thickness}$ chip thickness factor, C time coefficient, γ time exponent, k_B Boltzmann constant, α coffin-manson exponent. For the IGBT module in this work, the constants were obtained from [24] and [31].

The damage is given by [32],

$$\boldsymbol{Damage} = \sum \frac{\boldsymbol{N(\Delta T_j, T_m)}}{\boldsymbol{N_f(\Delta T_j, T_m)}} \quad (5)$$

where, N number of cycles in the region, N_f number of cycles to failure. Using (4) and (5), the degradation of IGBT for the given mission profiles is estimated. The amount of deterioration and RUL are estimated for various mission profiles, and the corresponding histograms are illustrated and discussed in section V.

IV. EXPERIMENTAL SETUP AND DATA COLLECTION

To validate the accuracy of the proposed inverter thermal analysis framework, the prototype of the three-phase induction motor drive system is utilized. The schematic of the proposed framework is shown in Fig. 7, which includes the major components and the signal flow between them.

A. EXPERIMENTAL PLATFORM

Fig. 7 and Fig. 8 depict the schematic of IoT based inverter health monitoring systems and their experimental arrangement respectively. The drive unit consists of a bridge rectifier module, DC link capacitors, and half-bridge IGBT modules (SKM100GB12T4), that are connected to the DC link of the drive system. To guarantee the secured operation of the inverter, the protection board is equipped. The protection board is integrated with hall-effect current and voltage sensors with the signal conditioning circuit that protects the circuit against short circuits and over-current. The protection board turns down the pulses supplied to the power module driver circuit under anomalous operation circumstances. The driver circuit (SKYPER 32 Pro), boosts the dSPACE controller output voltage (5 V and 0 V) to the gate switching voltage (15 V and - 15 V). The current sensor (HE055T01), speed sensor (HEDS-550), and torque transducers (from the load cell) are adapted for delivering inputs to the controller. On the other hand, a custom-built forced-air cooling heatsink

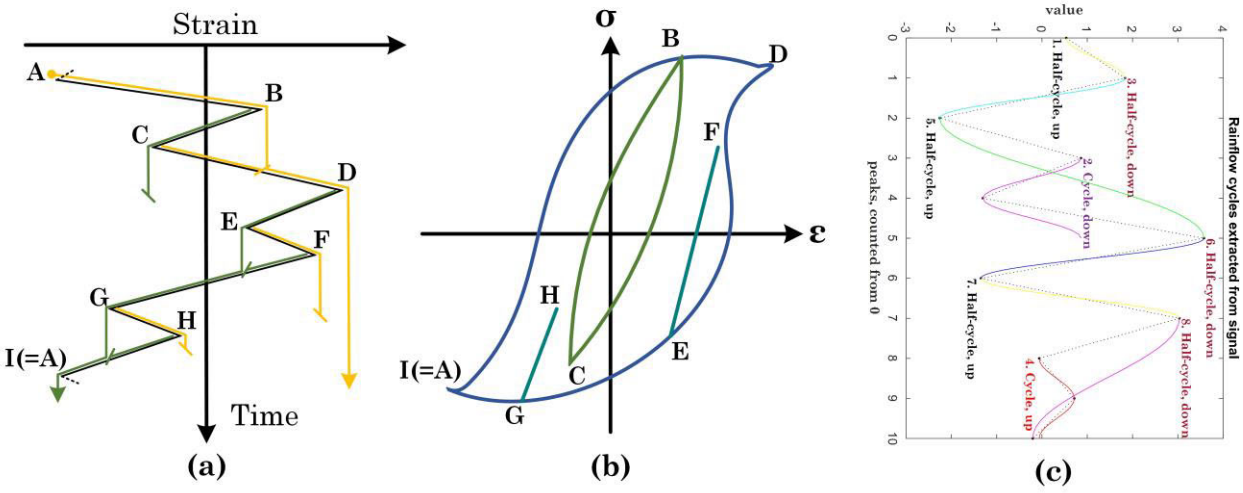

FIGURE 6. (a) Rainflow algorithm of cycle counting method. (b) Combine cycle events to form closed hysteresis loops (c) Rainflow algorithm of a signal with cycle's information from code available in MATLAB [26].

TABLE 1. Steps in rainflow algorithm.

If the rain flows from a peak: ✓ A to B to D then continues to the end. ✓ B to C stops at D ✓ C to D stops before D	*If the rain flows from the valley:* ✓ D to E to G and continues to the end ✓ E to F stops at G ✓ F stops before G ✓ G to H stops at I.
Combination of cycle events to form closed hysteresis loops (Fig.6 (b)): ✓ A to D cycle events are combined, which forms a complete cycle. ✓ B to C makes a complete cycle. ✓ E to F makes a partial cycle. ✓ G to H. forms a complete cycle. Similarly, Fig.6(c) shows the Rainflow algorithm of a signal with cycle information from code available in MATLAB.	

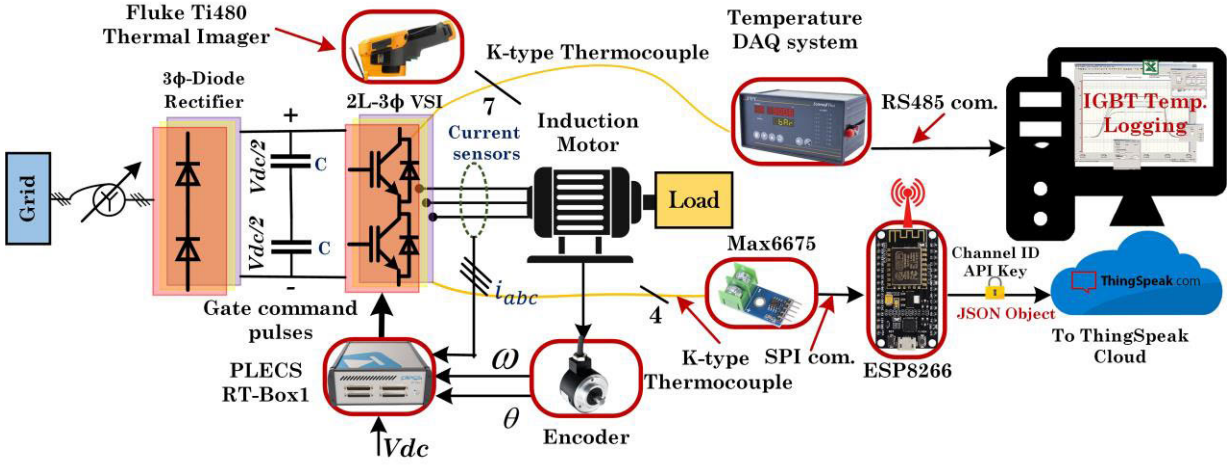

FIGURE 7. Schematic of IoT based IGBT switch module health monitoring system.

was developed to evacuate the junction temperature of IGBT under various operating conditions. A 3-phase, 3.7 kW (5 hp) induction motor is connected to the inverter output. The dSPACE MicroLabBox controller controls the induction motor drive through the PWM signals. The induction motor is mechanically integrated with a 3.7 kW (5 hp) DC generator

FIGURE 8. Real-time experimental setup.

TABLE 2. IM drive system specifications.

System Parameters	Symbols	Value
3-phase Induction Machine		
Rated power	P	3.7 kW
Rated speed	ω_m	150.8 rad/s
Rated torque	T_e	24.5 Nm
Base frequency	f	50 Hz
Motor poles pairs	p	2
Stator resistance	r_s	1.7639 Ω
Rotor resistance	r_r	1.0034 Ω
Stator leakage reactance	x_s	1.9040 Ω
Rotor leakage reactance	x_r	1.9040 Ω
Main reactance	x_h	71.6312 Ω
Iron loss resistance	r_{fe}	1379.226 Ω
Stator flux magnitude ref.	ψ_{si}	1 Wb
3-phase 2-Level VSI		
Power	S	10 kVA
Output Voltage	V	(0 to 415) V
DC-link voltage	V_{dc}	700 V
DC-link capacitors (2 Nos)	C	680 μF, 450 V
Semiconductor switch (IGBT)	$V_{CES} = 1200$ V, $I_C = 160$ A	

loading system. The 3-phase 2L-VSI based IM drive system parameters are tabulated in Table 2.

Furthermore, it ought to be noted that all three of the half-bridge IGBT modules include thermocouple probes placed beneath the case surface to estimate the junction temperature. To investigate the surface temperature of IGBT modules an IR camera is also utilized. It can display high-quality thermal images at 640 × 480 (307200 pixels) and has the specifications of spatial resolution of 0.93 mRad (milliradians), a minimum focus distance of 15 mm, temperature measurement ranges from −20°C to 1200°C and a 60 Hz frame rate. During heavy operating circumstances, the power dissipation of 3-phase 2L- VSI fluctuates significantly, leading to significant variations in junction temperature. Four tests with various load/mission profiles are set up to demonstrate the established improved RC model. The model can quickly and accurately predict the junction temperature under various operating circumstances. At the same time, using the PLECS software environment the Tj is extracted from the built RC model. The comparison of experimental results and estimation of junction temperature are discussed in section V.

B. IGBT MODULE CASE TEMPERATURE DATA LOGGING (TC)

The half-bridge IGBT module has four fast trench technology that can switch up to 20 kHz. It has a reverse blocking voltage of 1200 V and a maximum operating current of 100 A. It can operate reliably for case temperatures up to $T_c = 125°$ C and junction temperatures up to $T_j = 150°$ C. The temperature data of T_c is collected through thermocouple arrangement and junction temperature is estimated using (6) and validated with the proposed RUL method. The power cycling test has been conducted on the commercial IGBT power module (SKM100GB12T4) from SEMIKRON.

The IGBT switches (shown in Fig. 8) are triggered for different switching frequencies (f_{sw}) under different load conditions. This increases the IGBT junction temperature due to power loss and decreases in IGBT junction temperature due to heatsink in a regular interval. As a result, the IGBT switches experience significant thermomechanical stress, which will be reflected in the T_j. When the IGBT power module undergoes the power cycling test the average case temperature (T_c) is measured with the help of minimum junction temperature, recorded for every 10 seconds using a thermal scanner system and RS485 to USB converter. Every test set lasts for about 1000 seconds to monitor the junction temperature for the particular mission profile.

V. RESULTS AND VALIDATIONS

A. VALIDATION AND DISCUSSION OF TEST RESULTS

The proposed approach works twofold, in the first step real-time junction temperature data is collected from the experimental set-up to tune the thermal model implemented in the PLECS software environment. In the second step, the accuracy of the thermal model was validated by the operating model for various operating conditions and compared with the estimated junction temperature in the experimental setup. To confirm the exactness of the IGBT junction temperature calculations in PLECS, real-time measurement data are used. The case temperature T_c of the IGBT module is measured using thermocouples in order to estimate the T_j without opening it. To estimate junction temperature, the thermal impedance $R_{th(j-c)}$, value is collected from the datasheet.

Equation (6) is used to calculate temperature Tj:

$$T_j = R_{th(j-c)} \times P + T_c \tag{6}$$

Here,

$$\boldsymbol{P = I_{rms}^2 \times R_{ce}}$$

where P power loss of the IGBT, $R_{th(j-c)}$ thermal resistance between junction and case, R_{ce} the resistance between the collector and emitter. The loading profiles for the IGBT modules are determined using the suitable parameters of the IM drive.

In this research, the RC model for 3-phase 2L-VSI is applied in the PLECS environment for estimating the T_j. Considering the operating range of IM drive parameters, the junction temperature ($T_{j,RC}$) of IGBT modules are estimated and compared with experimental data for tuning the RC model. Fig. 9 shows the tuning procedure of the proposed thermal model. The experimental data is utilized for the curve fitting the data sheet curves (turn-ON/OFF energy as function (I_c) and transfer characteristic). In the next stage, the look-up tables (LUT) turn ON/turn OFF and conduction losses are updated. The thermal model simulation is performed in the PLECS environment, for estimating the junction temperature and comparing it with experimental data. The process is repeated until the relative error is less than or equal to the threshold value (δ_{th}). The comparison of experimental and simulation results is shown in Fig. 10. The quantitative consistency among the predicted T_j and the results of experimentation can be verified using the relative error. Definition of the relative error δ in (7):

$$\boldsymbol{\delta = \frac{\Delta T_{j,RC} - \Delta T_{j,Exp}}{\Delta T_{j,Exp}} X100\%} \tag{7}$$

The comparison results show a fair relation between the experimental and improved RC thermal models. Fig.10 (a) shows the changes in the junction temperature of IGBT during the torque variation in the IM drive. From Fig.10 (a), it is clear that the difference between simulations and experiments is reasonably less. Fig. 10(b) and 10(c) show junction temperatures as a function of the system switching frequency and speed of the IM drive. Here the error is comparatively greater because the system's current variation and harmonic contribution are high during switching frequency and speed variation.Fig.10(d) shows the variation in the junction temperature of the IGBT modules when the inverter operates in different DC-Link voltages. In this case, the difference between experimental and simulations is very less, because DC-Link voltage affects less in the current waveform in the closed loop system. Hence, the implemented thermal model of IGBT demonstrates improved accuracy. Fig. 11 shows the surface temperature distribution of IGBT modules captured by an IR camera when the IM drive system operates at an unloaded condition with a speed of 145 rad/s. The temperature spreading of power modules is inconsistent due to power dissipation and thermal coupling with dissipating boundary conditions. Under various loading scenarios, the power losses

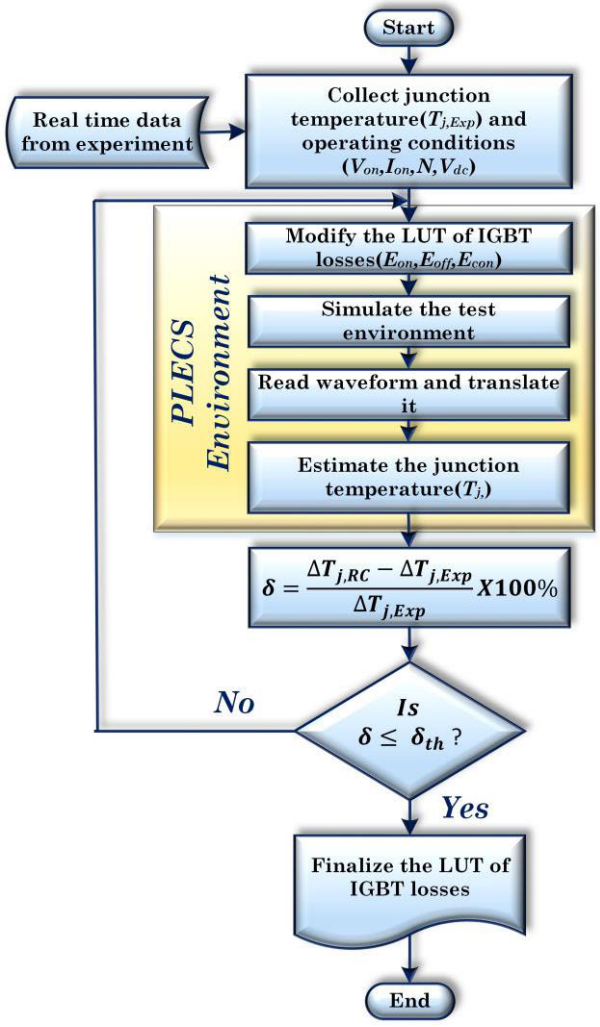

FIGURE 9. Proposed thermal model tuning procedure.

of the 3-phase 2L-VSI may vary significantly, leading to a significant change in T_j distribution.

1) THERMAL LOADING OF THE 3-PHASE 2L-VSI AT VARIOUS MISSION PROFILES

As illustrated in Fig. 12 to Fig.15, the mission profiles are designed based on various operating conditions of the inverter. The 3-phase 2L-VSI based IM drive system parameters for simulation are tabulated in Table 3. The test conditions for four types of mission profiles were designed to investigate the thermal stress experienced by SEMIKRON half-bridge-based 3-phase 2L-VSI. The power modules in motor drive applications normally undergo various operational parameter changes like speed, switching frequency, torque/load current, and DC-Link voltages. Hence, in this article mission profiles are designed accordingly to measure the thermal stress of the VSI inverter and also to find the RUL of the inverter during different operating conditions. Fig. 12(a) illustrates stator current (rms), speed, DC link voltage, and IGBT junction temperature variation for different torque conditions. In this

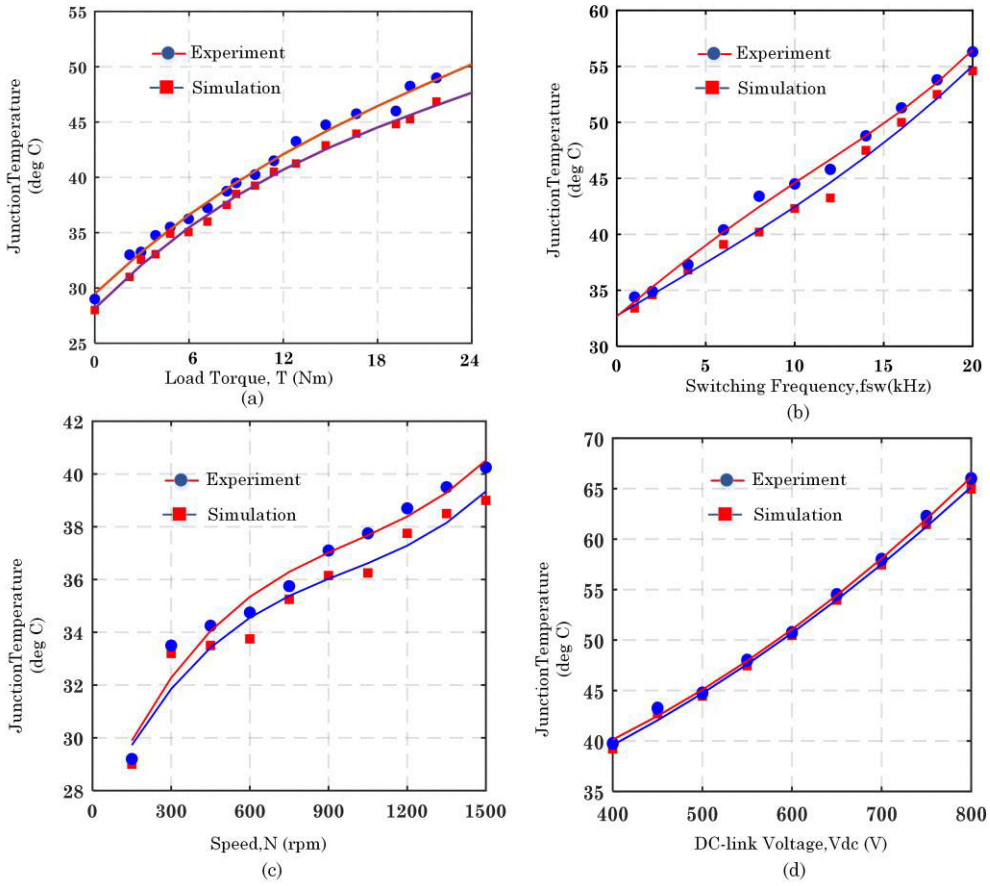

FIGURE 10. Experimental and simulation relative analysis, (a) Torque variation, (b) Switching Frequency variation, (c) Speed variation, (d) DC link voltage variation.

mission profile I, the speed is maintained at 130 rad/s, the DC-link voltage is 650 V, the switching frequency is kept constant at 10 kHz and the torque is varied from 10 to 160 Nm. The cycle counting algorithm takes the thermal stress profile (Junction temperature of IGBT) of the 3-phase 2L-VSI as input data. The rainflow algorithm decomposes the temperature swing range (ΔTj), average temperature Tjm, and corresponding cycle depths and averages. Fig. 12(b) shows the histogram output of the junction temperature profile input. From Fig. 12 (b), it is evident that the highest number of cycles (10000 cycles) occurred at a mean temperature of 48°C in the IGBT switches during the mission profile-I operation. Also, Fig.12 (b) depicts that 10000 cycles of the mean value of junction temperature are spread across 40°C to 80°C. Similarly, Fig. 12(b) shows that the change in junction temperature is distributed over the range of 0°C to 10°C. The exact number of cycles depends on the stress imposed on the IGBT switch during the mission profile operation. Which is a strong candidate for the deterioration of the IGBT modules.

As shown in Fig. 13(a), mission profile-II is designed for a constant speed of 130 rad/s, DC-Link voltage is 650 V, the load torque is kept constant at 80 Nm and the switching frequency is varied from 1 to 20 kHz. Fig. 13(b) shows the histogram output of the junction temperature profile input. From Fig. 13(b), it is evident that the highest number of cycles (8000 cycles) occurred at a mean temperature of 44°C in the IGBT switches during the mission profile II operation. Also, Fig. 13(b) depicts that 8000 cycles of the mean value of junction temperature are spread across 35°C to 80°C. Similarly, Fig. 13(b) shows that the change in junction temperature is distributed over the range of 0°C to 15°C. Which is the second highest among four mission profiles designed for the system under test. Similarly, Fig. 14(a) depicts the stator current (rms), speed, DC-link voltage, and IGBT junction temperature variation for different speed conditions. In this mission profile-II, the DC-Link voltage is kept at 650 V, the switching frequency is maintained constant at 10 kHz, the torque remains at 80 nm and the speed is varied from 10 to 145 rad/s. Fig. 14(b) shows the histogram output of the junction temperature profile input. From Fig. 14(b), it is evident that the highest number of cycles (7000 cycles) occurred at a mean temperature of 20°C in the IGBT switches during the mission profile-III operation. Also, Fig. 14(b) depicts that 7000 cycles of the mean value of junction temperature are spread across 0°C to 90°C. But most of the histogram accumulated towards under 40°C. Similarly, Fig. 14(b) shows that the change in

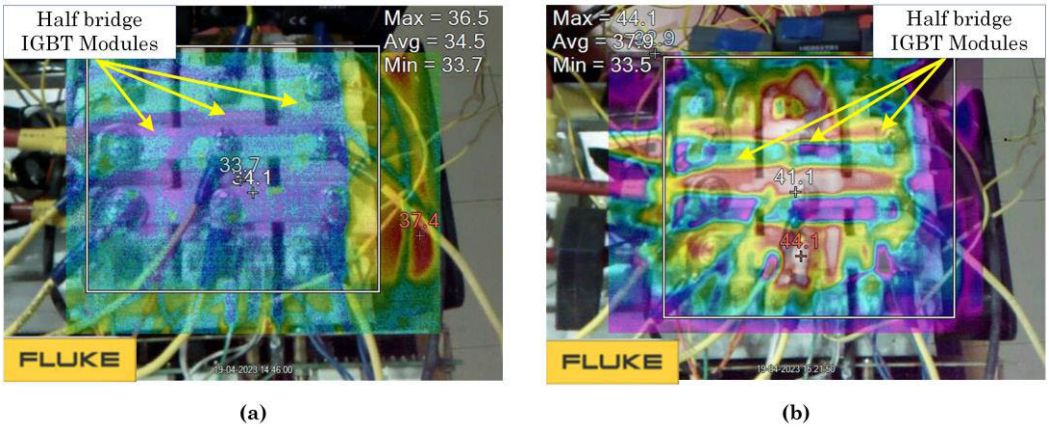

FIGURE 11. Temperature distribution of inverter caught by IR camera; (a) unloaded condition, (b) loaded condition.

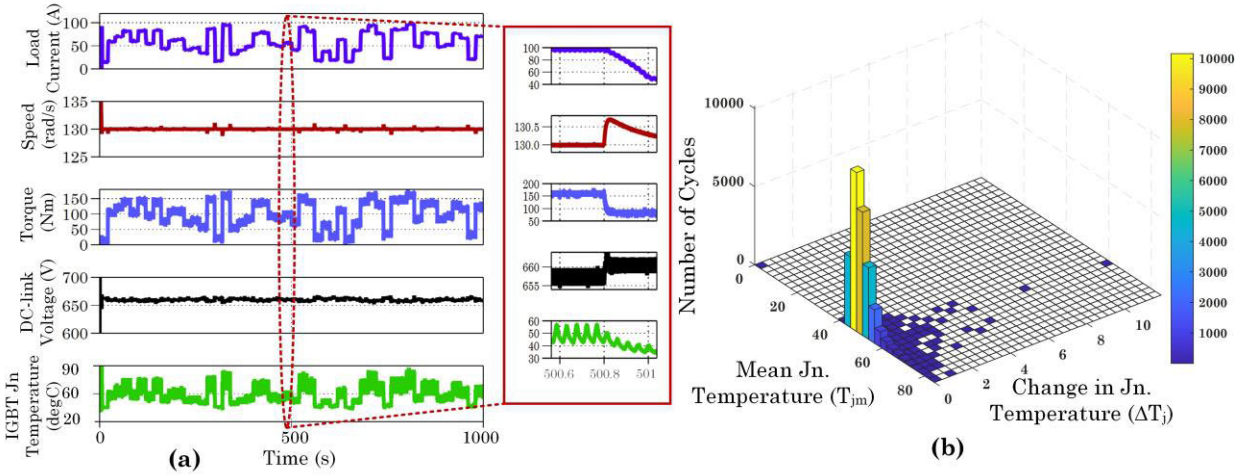

FIGURE 12. Mission profile-I (a)IM drive parameters as function of torque variation (b) Results of the mission profile's rainflow cycle counting (Histogram) for the number of cycles (Ni), average junction temperature Tjm (C), and change in junction temperature Δ Tj (C).

junction temperature is distributed over the range of 0°C to 60°C. Finally, mission profile-IV is shown in Fig. 15 (a), here the speed of IM is maintained at 130 rad/s, the switching frequency is kept at 10 kHz, the torque remains 80 Nm and the DC-Link voltage is varied between 400 V to 800 V. Fig. 15(b) shows the histogram output of the junction temperature profile input. From Fig. 15(b), it is evident that the highest number of cycles (4000 cycles) occurred at a mean temperature of 18°C in the IGBT switches during the mission profile-III operation. Also, Fig.15(b) depicts that 4000 cycles of the mean value of junction temperature are spread across 0°C to 50°C. But most of the histogram accumulated towards under 40°C. Similarly, Fig. 15(b) shows that the change in junction temperature is distributed over the range of 0°C to 33°C. Hence from Fig. 12 to Fig. 15, it is obvious that load current/torque variation and switching frequency variation create a major impact on the IGBT module lifetime. The next section details the effect of mission profiles on the RUL and the percentage of damage to IGBT modules. Also, Table – 4 summarizes RUL variation with different operating conditions and different parameters.

B. LIFETIME ESTIMATION OF IGBT IN INDUCTION MOTOR DRIVE APPLICATIONS

The IGBT module undergoes major thermal stresses during load torque variation and switching frequency variation. To determine the remaining useful lifetime of IGBT modules, the rain flow algorithms are adapted. As explained in section III, (9) and (10) are used to estimate RUL and percentage of power modules. It can be seen from Fig. 16(a), that for the maximum value load torque, the IGBT module's lifetime is considerably decreased due high amount of losses in the semiconductor device. The variation in torque will directly impact the inverter load current hence this will increase the conduction losses, consecutively increasing the thermal stress on the IGBT devices. This is evident in the percentage damage accumulation in Fig. 16(a).

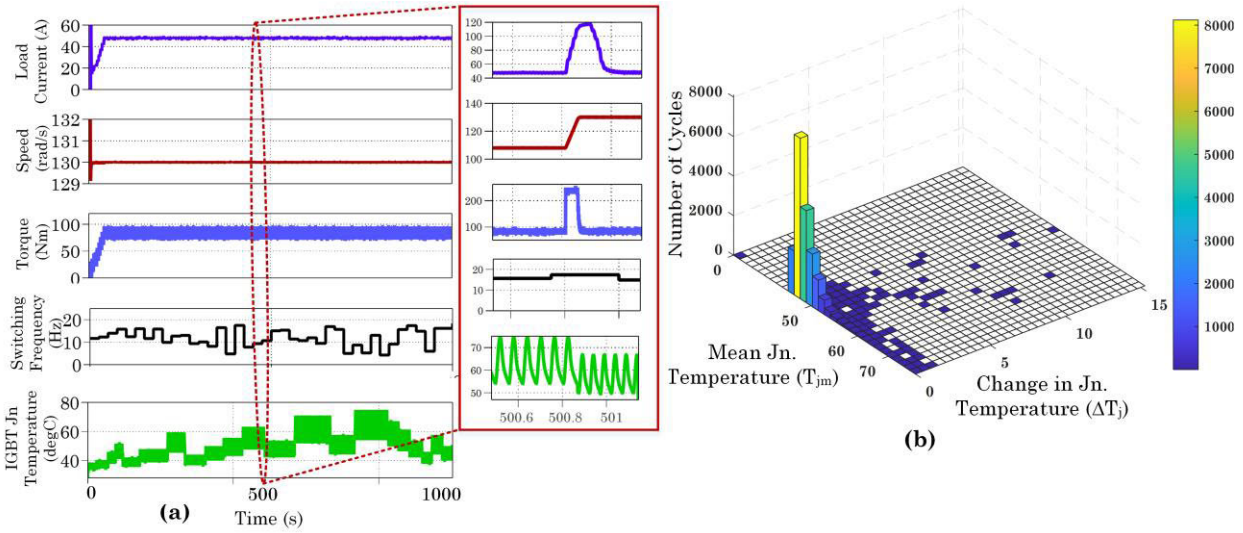

FIGURE 13. Mission profile-II (a)IM drive parameters as function of torque variation (b) Results of the mission profile's rainflow cycle counting (Histogram) for the number of cycles (Ni), average junction temperature Tjm (C), and change in junction temperature Δ Tj (C).

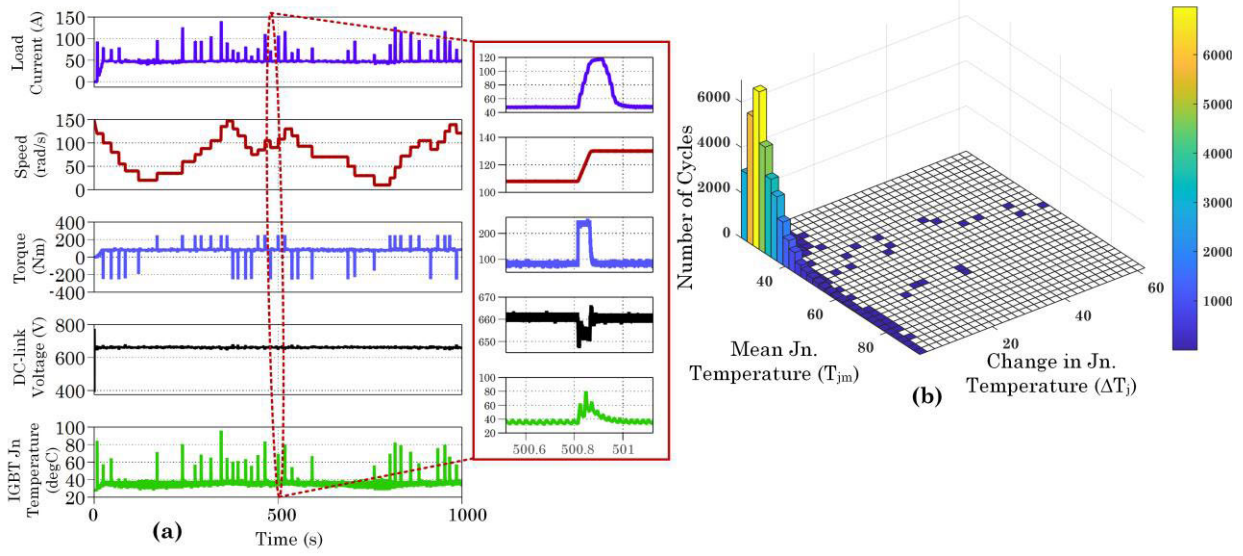

FIGURE 14. Mission profile-III (a)IM drive parameters as function of torque variation (b) Results of the mission profile's rainflow cycle counting (Histogram) for the number of cycles (Ni), average junction temperature Tjm (C), and change in junction temperature Δ Tj (C).

Similarly, Fig. 16(b) to Fig. 16(d) shows the impact of various switching frequencies, speed, and DC-link voltage variations on the RUL of the inverter motor drive applications. From Fig. 16(b), it is clear that switching frequency variation deteriorates the IGBT modules in a reasonable amount due to heavy switching losses during higher frequencies. The RUL and percentage of damage are shown in Fig. 16(c) for speed variation which is comparatively less when considering load torque and switching frequency variation. Because the speed variation does not affect the current or switching frequency of the inverter. Because current and switching frequency are the major components for the loss of IGBT devices. For the case of DC-Link variation of IM drive, which has similar effects on the IGBT modules, which is evident in Fig. 16(d).

The proposed method combines real-time data fetching for thermal model correction in the PLECS environment for accuracy improvement. Thence the related works in the literature are compared and tabulated in Table 5. In [18], [33], [34], and [35] various approaches are presented for RUL estimation, but all these works have not considered the dynamic loading with electrical motors. Hence, those approaches on RUL estimated will not be in good agreement with real-time operating conditions. In [33], the key contribution is to link the physics of the power switches with a power converter

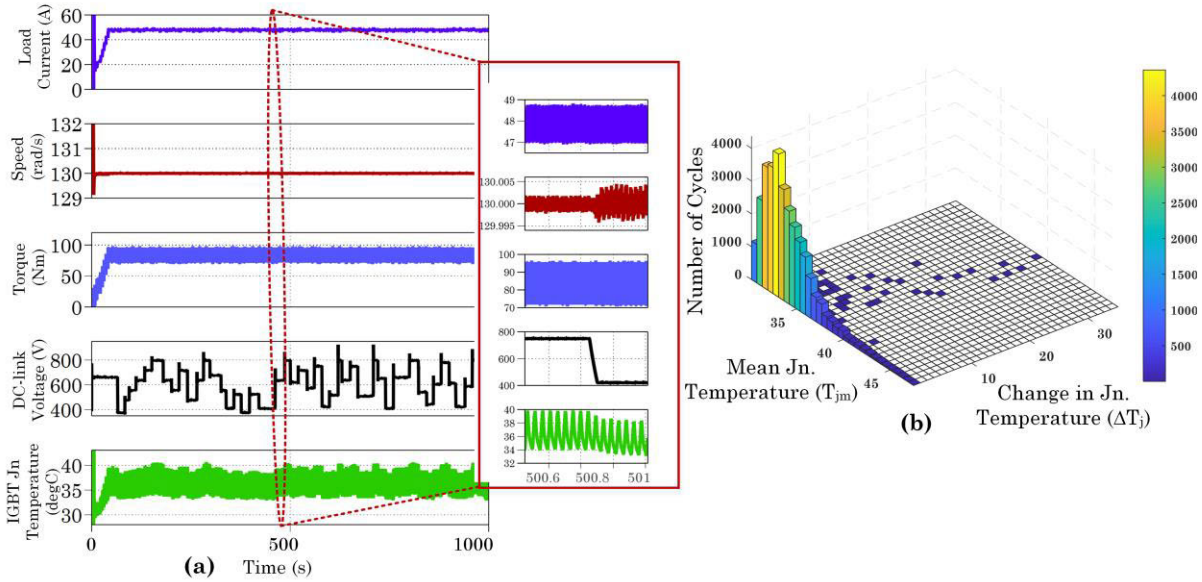

FIGURE 15. Mission profile-IV (a)IM drive parameters as function of torque variation (b) Results of the mission profile's rainflow cycle counting (Histogram) for the number of cycles (Ni), average junction temperature Tjm (C), and change in junction temperature Δ Tj (C).

simulation model. By applying this method to a real system, a converter design tool or online lifespan prediction tool may be built. This eventually results in an inference that die-attach solder fatigue is the most common failure mode of this IGBT module under its intended accelerated testing. Rainflow algorithms are a prominent counting method used in fatigue and failure analysis along with lifespan prediction models. The Rainflow technique employed in power semiconductor reliability does not account for time-dependent mean temperature assessments. Hence, in [34] a modified Rainflow algorithm is proposed that is based on time-dependent mean calculation of temperature. Similarly, the equivalent temperature calculation is proposed and applied to semiconductor lifetime estimation in [36]. However, the inverter connected to the motor load will undergo different dynamic conditions. In [35], electro-thermal models are combined with physics-of-failure analysis via the real-time counting technique to offer realistic life consumption estimates for power modules running in service. In [18], the ON-state voltage (V_{CE-ON}) of the IGBT varies as the fracture propagates, and the history of V_{CE-ON} is utilized to forecast the remaining useable lifespan. The particle-based marginalized resample-move method can estimate the length of bond wire cracks. However the major shortcoming of this method is during real-time operating conditions, it is hard to measure mV range variation V_{CE-ON} due to device degradation to estimate the RUL. Similarly, in [36] and [37] the authors discuss the reliability forecasting techniques for capacitor banks in electric vehicles. In [36], online learning long short-term memory (LSTM) and fault-detection method proposed, which adapts the sudden internal CB faults with the LSTM to correctly predict the CB degradation. An improved method proposed in [37], a novel formula is introduced to estimate the reliability and lifetime of CBs, while an existing formula for calculating CB peak output current is enhanced. By considering all the above methods, the proposed method utilizes the thermal model which is tuned with real-time operating data under various operating conditions of electric drive. Once the thermal model T_j matches with real-time data, using the normal motor's parameters (torque, speed, switching frequency, and DC-link voltage) is sufficient to estimate the RUL during a real-time operating environment. Also, most of the thermal model improvement methods did not consider the dynamic operating conditions of the inverter-based motor drives RUL is also not estimated during transient operating conditions. In contrast, the proposed scheme investigated the RUL (years) and damage of the inverter IM motor drive operating in various mission/load profiles.

TABLE 3. IM drive system specifications for simulation.

System Parameters	Symbols	Value
3-phase Induction Machine		
Rated power	P	23 kW
Rated speed	ω_m	150.8 rad/s
Rated torque	T_e	152.5 Nm
Base frequency	f	50 Hz
Motor poles pairs	p	2
Stator resistance	r_s	0.08233 Ω
Rotor resistance	r_r	0.0503 Ω
Stator leakage reactance	x_s	0.225888 Ω
Rotor leakage reactance	x_r	0.225888 Ω
Main reactance	x_h	8.51254 Ω
Stator flux magnitude ref.	ψ_{si}	0.95 Wb

C. IOT BASED INVERTER JUNCTION TEMPERATURE MONITORING

The utilization of IoT and AI technologies is increasingly prevalent in smart grid systems, transportation electrification,

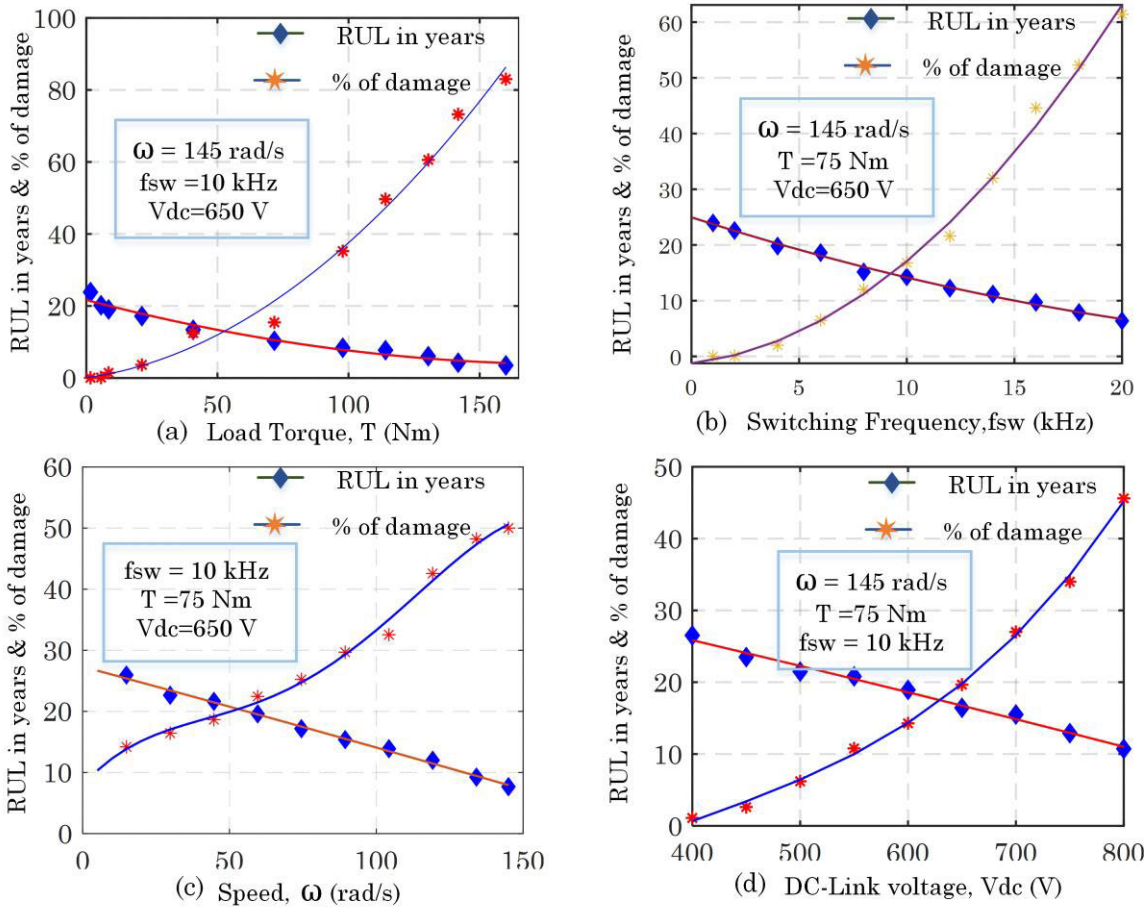

FIGURE 16. RUL (in years) and percentage of damage as function of (a) load torque (b) switching frequency (c) speed (d) DC link voltage.

TABLE 4. Effects of operational parameters on RUL of inverter.

Remaining Useful Lifetime (RUL) in Years	Operational Parameters							
	Load Torque, T (Nm)				Switching Frequency, fsw (kHz)			
	0	75	120	150	2	10	15	20
	23.8468	13.3995	7.7259	3.4999	23.955	14.282	9.7019	6.3772
	Speed, ω (rad/s)				DC-Link Voltage, Vdc (V)			
	20	70	115	148	400	550	670	800
	20.947183	14.5895	9.9976	4.2944	26.517	18.9319	15.5046	10.7259

and related areas. These technologies facilitate more accurate assessments of the State of Health (SOH) of devices. This involves real-time monitoring of the power converter while it is in operation. Beyond its technical aspects, IIoT embodies a transformative business model, enabling users to access applications remotely via the cloud without the need for local installation, thereby facilitating seamless file and document management from any location. The IoT cloud-based condition monitoring is implemented as the extension of the proposed work, through which the user/operator will receive an Email/SMS notification when the temperature of IGBT modules exceeds the pre-set critical temperature of the operating condition. ThingSpeak is a public cloud platform for IoT data that was selected to monitor the temperature of an inverter IGBT module. It has an open API that allows for real-time data collection, analysis, and action. The most important feature of ThingSpeak is its 'Channel' component, which has fields for data, location, and status.

TABLE 5. Performance comparison with existing work.

Reference	Methodology	Lifetime model	Failure Mechanism	No.of mission profiles considered
Huang *et.al* [33]	Power cycling test based lifetime data	Modified Coffin–Manson law	Solder fatigue	One (Wind turbine application)
GopiReddy *et.al* [34]	Modified Rainflow algorithm	Arrhenius-Coffin-Manson's lifetime model	Bond wire	One (STATCOM for reactive compensation)
M. Musallam *et.al* [35]	Thermomechanical Models (Damage Models)	Improved Coffin–Manson law	Bond-wire and Solder fatigue	Two (Metro-system and wind-turbines applications)
Keting Hu *et.al* [18]	ON-state voltage of IGBT	Fusion of model-driven and data-driven approach	Bond-wire liftoff	No (Accelerated power cycling test)
Proposed method	**Modified electro-thermal model**	**SKiM63 (Scheuermann et. al.)**	**Bond-wire and Solder fatigue**	**Four types of EV mission profiles**

In this work, once a channel is created, using ESP8266 that data can be added to the channel and further processed and visualized. Alerts such as tweets can also be triggered in response to the data. Fig. 17(a-d) shows real-time temperature data from an ESP8266 WiFi module sent to a ThingSpeak cloud channel field. The case temperature of a SEMIKRON IGBT half-bridge module is measured using a K-type thermocouple connected to a MAX6675 thermocouple sensor module and the junction temperature is estimated using (11) in an ESP8266 controller. The temperatures of three IGBT modules and a heat sink are monitored in four fields of the inverter temperature monitoring channel. ThingSpeak server updates the temperature data every 15 seconds with real-time data and the channel fields are written by making API requests to the ThingSpeak API using a unique write key. Fig. 17(e) shows the email received using the ThingSpeak cloud when the system detects an IGBT module temperature exceeds the critical temperature set by the user/operator. Based on the mail notification the user can make critical decisions like either shutdown the system or operating in light load conditions to avoid further damage to the IM drive system.

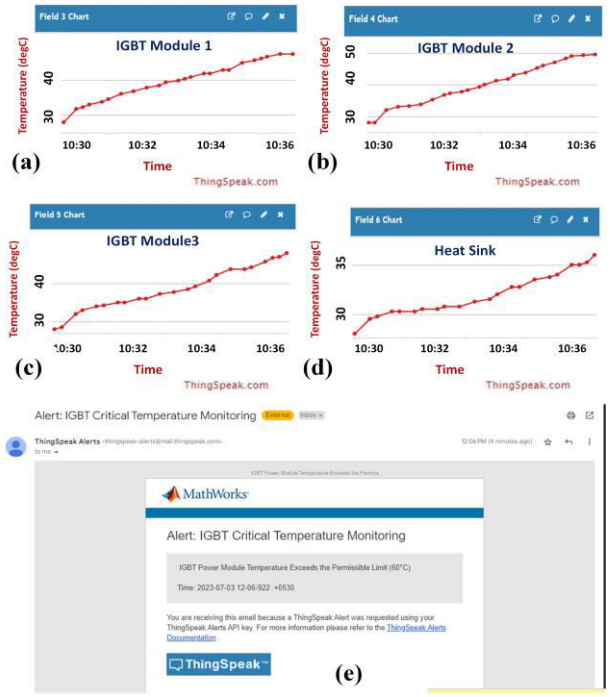

FIGURE 17. (a)-(d) Real-time junction temperature monitoring of 3-IGBT module and Heat sink on IoT cloud (e) Email alert sent by ThingSpeak upon critical temperature.

VI. GRAPHICAL USER INTERFACE FOR RUL ESTIMATION

The proposed work was further extended to enhance reliability and condition monitoring. Fig. 17 shows a Matlab based RUL estimation application that has been developed to make the proposed work user-friendly. The designed user interface of the MATLAB application mainly includes two parts: The input section and the output section as illustrated in Fig. 18. The Input section has four sub-sections load mission profile, plot data, profile period, and change in junction temperature. Load mission profile accepts the mission profile data in the form of an Excel file. Once the mission profile is loaded, the corresponding plot can be plotted when the plot data tab is pressed. Apart from mission profile data, this app needs two parameters that are period of mission (in sec) and the change in junction temperature, ΔTj. These two pieces of information can be passed to the app through the numeric input section ''profile period'' and ''change in junction temperature''. The output section includes three subsections namely the estimate RUL tab, RUL (in days), and RUL (in years) display sections. After passing the necessary information in the input section of the app estimate RUL has to be pressed to obtain the remaining useful life of the inverter for the particular mission profile.

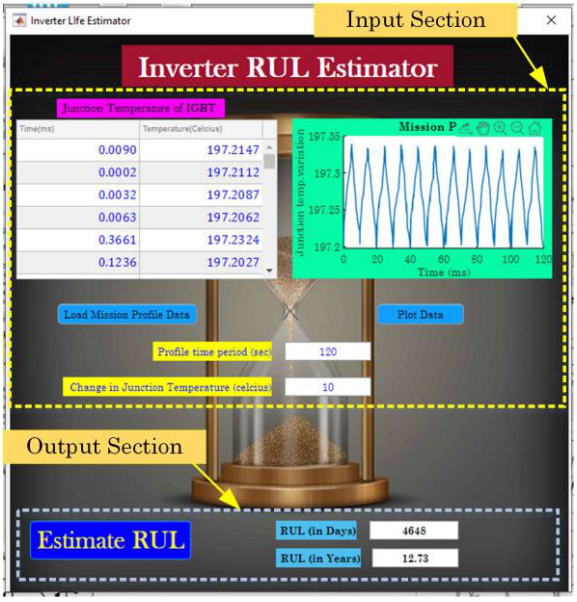

FIGURE 18. MATLAB GUI to estimate the remaining useful lifetime of 3-phase 2L-VSI inverter.

VII. CONCLUSION AND FUTURE WORK

Induction motor drives are the most popular in various drive-based applications due to their better performance and lower maintenance. For IM motor drives, a strong prognosis and health management structure are crucial due to the rising demand and complex operating environment. Power semiconductors (IGBT) are a crucial and sensitive component in IM motor drive applications, and their reliability has gained significant research attention. From the remaining useful life estimation and damage percentage perspective, it is clear that load current and switching frequency variations persuade for the system damage. In the case of load current variation, the device deterioration value reaches up to 80 % for the load current of 150 A. Similarly, when the switching frequency varied from 1 kHz to 20 kHz the deterioration reached the maximum of 63 %. However, the variation of other parameters such as speed and DC-link voltage are less dominant in deteriorating the system. The percentage of deterioration for speed and DC-link voltage is 50 and 45 respectively. From this, the authors conclude that load current (torque) and switching frequency variations highly influence the remaining life of power devices. From the comparison of existing work, it is clear that the proposed work is superior in performance. It gives an accurate prediction of a lifetime since it considers the dynamic conditions of the electric drives. The proposed work is compared with the existing works, which indicates that Based on these results, as future work suitable algorithms can be investigated to optimize the operation drive system to increase the RUL of the system.

A simple user-friendly Matlab GUI-based application developed to estimate the inverter's lifetime based on temperature profiles provided. IoT-based computing appears as the best option for condition monitoring of power converters operating at different sites as a result of the evident advantages of online storage, collection of data, the integration of many services, and flexibility. As an outcome, particularly for mission-critical scenarios, the work shown here increases the reliability of the power converter system. In the future, this work can be extended for intelligent power modules (IPM) where more IGBT and diodes are integrated with a single module to realize the power electronic converters. Also, the RUL data for different operating conditions can be further utilized to train the machine learning model to implement the RUL estimation for the given real-time operating condition.

ACKNOWLEDGMENT

The research work has been carried out in Advanced Drives Laboratory, School of Electrical Engineering. The Vellore Institute of Technology, Vellore is acknowledged by the authors for providing research facilities and funds for this research.

REFERENCES

[1] E. Zio, "Prognostics and health management (PHM): Where are we and where do we (need to) go in theory and practice," *Rel. Eng. Syst. Saf.*, vol. 218, Feb. 2022, Art. no. 108119, doi: 10.1016/j.ress.2021.108119.

[2] R. Wu, F. Blaabjerg, H. Wang, M. Liserre, and F. Iannuzzo, "Catastrophic failure and fault-tolerant design of IGBT power electronic converters—An overview," in *Proc. IECON - 39th Annu. Conf. IEEE Ind. Electron. Soc.*, Nov. 2013, pp. 507–513, doi: 10.1109/IECON.2013.6699187.

[3] R. Manikandan, S. Raghu, and R. R. Singh, "An improved open switch fault diagnosis strategy for variable speed drives," in *Proc. IEEE Int. Conf. Power Electron., Smart Grid, Renew. Energy (PESGRE)*, Jan. 2022, pp. 1–6, doi: 10.1109/PESGRE52268.2022.9715936.

[4] C. Fang, T. An, F. Qin, X. Bie, and J. Zhao, "Study on temperature distribution of IGBT module," in *Proc. 18th Int. Conf. Electron. Packag.*, 2017, pp. 1–24.

[5] D. Zhao, C. Guo, Y. Li, S. Pan, S. Feng, and H. Zhu, "Study of the temperature distribution in insulated gate bipolar transistor module under different test conditions," *Microelectron. Rel.*, vol. 140, Jan. 2023, Art. no. 114880, doi: 10.1016/j.microrel.2022.114880.

[6] C. Neeb, L. Boettcher, M. Conrad, and R. W. De Doncker, "Innovative and reliable power modules: A future trend and evolution of technologies," *IEEE Ind. Electron. Mag.*, vol. 8, no. 3, pp. 6–16, Sep. 2014, doi: 10.1109/MIE.2014.2304313.

[7] A. Abuelnaga, M. Narimani, and A. S. Bahman, "A review on IGBT module failure modes and lifetime testing," *IEEE Access*, vol. 9, pp. 9643–9663, 2021, doi: 10.1109/ACCESS.2021.3049738.

[8] B. Wang, J. Cai, X. Du, and L. Zhou, "Review of power semiconductor device reliability for power converters," *CPSS Trans. Power Electron. Appl.*, vol. 2, no. 2, pp. 101–117, 2017, doi: 10.24295/CPSSTPEA.2017.00011.

[9] D. Xiang, L. Ran, P. Tavner, S. Yang, A. Bryant, and P. Mawby, "Condition monitoring power module solder fatigue using inverter harmonic identification," *IEEE Trans. Power Electron.*, vol. 27, no. 1, pp. 235–247, Jan. 2012, doi: 10.1109/TPEL.2011.2160988.

[10] M. Ciappa, "Selected failure mechanisms of modern power modules," *Microelectron. Rel.*, vol. 42, nos. 4–5, pp. 653–667, Apr. 2002, doi: 10.1016/s0026-2714.

[11] G. Zeng, L. Borucki, O. Wenzel, O. Schilling, and J. Lutz, "First results of development of a lifetime model for transfer molded discrete power devices," in *Proc. PCIM Eur. Int. Exhibition. Conf. Power Electron., Intell. Motion, Renew. Energy Energy Manage.*, Jun. 2018, pp. 1–8.

[12] A. Vaccaro, P. Magnone, A. Zilio, and P. Mattavelli, "Predicting lifetime of semiconductor power devices under power cycling stress using artificial neural network," *IEEE J. Emerg. Sel. Topics Power Electron.*, vol. 11, no. 6, pp. 5626–5635, Jul. 2022, doi: 10.1109/JESTPE.2022.3194189.

[13] N. Dornic, Z. Khatir, S. H. Tran, A. Ibrahim, R. Lallemand, J.-P. Ousten, J. Ewanchuk, and S. V. Mollov, "Stress-based model for lifetime estimation of bond wire contacts using power cycling tests and finite-element modeling," *IEEE J. Emerg. Sel. Topics Power Electron.*, vol. 7, no. 3, pp. 1659–1667, Sep. 2019, doi: 10.1109/JESTPE.2019.2918941.

[14] M. A. Miner, "Cumulative damage in fatigue," *J. Appl. Mech.*, vol. 12, no. 3, pp. A159–A164, Sep. 1945, doi: 10.1115/1.4009458.
[15] P. D. Reigosa, H. Wang, Y. Yang, and F. Blaabjerg, "Prediction of bond wire fatigue of IGBTs in a PV inverter under a long-term operation," *IEEE Trans. Power Electron.*, vol. 31, no. 10, pp. 7171–7182, Oct. 2016, doi: 10.1109/TPEL.2015.2509643.
[16] J. Lutz, H. Schlangenotto, U. Scheuermann, and R. De Doncker, "Destructive mechanisms in power devices," in *Semiconductor Power Devices: Physics, Characteristics, Reliability*, 2nd ed., New York, NY, USA: Springer,2011, ch. 13, sec. 13.1, pp. 583–586.
[17] A. Hanif, Y. Yu, D. DeVoto, and F. Khan, "A comprehensive review toward the state-of-the-art in failure and lifetime predictions of power electronic devices," *IEEE Trans. Power Electron.*, vol. 34, no. 5, pp. 4729–4746, May 2019, doi: 10.1109/TPEL.2018.2860587.
[18] K. Hu, Z. Liu, H. Du, L. Ceccarelli, F. Iannuzzo, F. Blaabjerg, and I. A. Tasiu, "Cost-effective prognostics of IGBT bond wires with consideration of temperature swing," *IEEE Trans. Power Electron.*, vol. 35, no. 7, pp. 6773–6784, Jul. 2020, doi: 10.1109/TPEL.2019.2959953.
[19] D. Astigarraga, F. M. Ibanez, A. Galarza, J. M. Echeverria, I. Unanue, P. Baraldi, and E. Zio, "Analysis of the results of accelerated aging tests in insulated gate bipolar transistors," *IEEE Trans. Power Electron.*, vol. 31, no. 11, pp. 7953–7962, Nov. 2016, doi: 10.1109/TPEL.2015.2512923.
[20] A. Vaccaro, D. Biadene, and P. Magnone, "Remaining useful lifetime prediction of discrete power devices by means of artificial neural networks," *IEEE Open J. Power Electron.*, vol. 4, no. 9, pp. 978–986, Jul. 2023, doi: 10.1109/OJPEL.2023.3331814.
[21] M. Hernes, S. D'Arco, A. Antonopoulos, and D. Peftitsis, "Failure analysis and lifetime assessment of IGBT power modules at low temperature stress cycles," *IET Power Electron.*, vol. 14, no. 7, pp. 1271–1283, May 2021, doi: 10.1049/pel2.12083.
[22] F. Wani, U. Shipurkar, J. Dong, H. Polinder, A. Jarquin-Laguna, K. Mostafa, and G. Lavidas, "Lifetime analysis of IGBT power modules in passively cooled tidal turbine converters," *Energies*, vol. 13, no. 8, p. 1875, Apr. 2020, doi: 10.3390/en13081875.
[23] S. Chakraborty, M. M. Hasan, M. Paul, D.-D. Tran, T. Geury, P. Davari, F. Blaabjerg, M. E. Baghdadi, and O. Hegazy, "Real-life mission profile-oriented lifetime estimation of a SiC interleaved bidirectional HV DC/DC converter for electric vehicle drivetrains," *IEEE J. Emerg. Sel. Topics Power Electron.*, vol. 10, no. 5, pp. 5142–5167, Oct. 2022, doi: 10.1109/JESTPE.2021.3083198.
[24] Z. Luo, H. Ahn, and M. A. E. Nokali, "A thermal model for insulated gate bipolar transistor module," *IEEE Trans. Power Electron.*, vol. 19, no. 4, pp. 902–907, Jul. 2004, doi: 10.1109/tpel.2004.830089.
[25] P. Górecki and D. Wojciechowski, "Accurate computation of IGBT junction temperature in PLECS," *IEEE Trans. Electron Devices*, vol. 67, no. 7, pp. 2865–2871, Jul. 2020, doi: 10.1109/TED.2020.2992233.
[26] S. Balanethiram, A. Chakravorty, R. D'Esposito, S. Fregonese, D. Céli, and T. Zimmer, "Accurate modeling of thermal resistance for on-wafer SiGe HBTs using average thermal conductivity," *IEEE Trans. Electron Devices*, vol. 64, no. 9, pp. 3955–3960, Sep. 2017, doi: 10.1109/TED.2017.2724939.
[27] A. Wintrich, U. Nicolai, W. Tursky, and T. Reimann, *Application Manual Power Semiconductors*, 2nd ed., Nuremberg, Germany: Semikron International GmbH, 2015, pp. 279–294.
[28] M. Matsuishi and T. Endo, "Fatigue of metals subjected to varying stress," Presented at the Japan Soc. Mech. Eng., Fukuoka, Japan, Mar. 1968.
[29] A. Nieslony. (2024). *Rainflow Counting Algorithm*. MATLAB Central File Exchange. Accessed: Aug. 15, 2024. [Online]. Available: https://www.mathworks.com/matlabcentral/fileexchange/3026-rainflow-counting-algorithm
[30] M. Held, P. Jacob, G. Nicoletti, P. Scacco, and M.-H. Poech, "Fast power cycling test of IGBT modules in traction application," in *Proc. 2nd Int. Conf. Power Electron. Drive Syst.*, vol. 1, pp. 425–430, doi: 10.1109/peds.1997.618742.
[31] R. Bayerer, T. Herrmann, T. Licht, J. Lutz, and M. Feller, "Model for power cycling lifetime of IGBT modules–various factors influencing lifetime," in *Proc. 5th Int. Conf. Integr. Power Electron. Syst.*, Mar. 2008, pp. 1–6.
[32] M. H. Aliabadi, "Fundamentals of metal fatigue analysis," *Eng. Anal. Boundary Elements*, vol. 9, no. 3, p. 280, Jan. 1992, doi: 10.1016/0955-7997.
[33] H. Huang and P. A. Mawby, "A lifetime estimation technique for voltage source inverters," *IEEE Trans. Power Electron.*, vol. 28, no. 8, pp. 4113–4119, Aug. 2013, doi: 10.1109/TPEL.2012.2229472.
[34] L. R. GopiReddy, L. M. Tolbert, B. Ozpineci, and J. O. P. Pinto, "Rainflow algorithm-based lifetime estimation of power semiconductors in utility applications," *IEEE Trans. Ind. Appl.*, vol. 51, no. 4, pp. 3368–3375, Jul. 2015, doi: 10.1109/TIA.2015.2407055.
[35] M. Musallam, C. Yin, C. Bailey, and M. Johnson, "Mission profile-based reliability design and real-time life consumption estimation in power electronics," *IEEE Trans. Power Electron.*, vol. 30, no. 5, pp. 2601–2613, May 2015, doi: 10.1109/TPEL.2014.2358555.
[36] M. A. Rezaei, A. Fathollahi, S. Rezaei, J. Hu, M. Gheisarnejad, A. R. Teimouri, R. Rituraj, A. H. Mosavi, and M.-H. Khooban, "Adaptation of a real-time deep learning approach with an analog fault detection technique for reliability forecasting of capacitor banks used in mobile vehicles," *IEEE Access*, vol. 10, pp. 132271–132287, 2022, doi: 10.1109/ACCESS.2022.3228916.
[37] M. A. Rezaei, "Reliability calculation improvement of electrolytic capacitor banks used in energy storage applications based on internal capacitor faults and degradation," *IEEE Access*, vol. 12, pp. 13146–13164, 2024, doi: 10.1109/ACCESS.2024.3351604.

R. MANIKANDAN received the B.E. degree in electrical and electronics engineering from Bharathidasan University, Tiruchirappalli, India, in 2003, and the M.E. degree in VLSI design from Anna University, Chennai, India, in 2008. He is currently pursuing the Ph.D. degree in power electronics systems with the School of Electrical Engineering, Vellore Institute of Technology (VIT), Vellore, India. His research interests include fault diagnosis, remain useful lifetime (RUL) estimation of power electronics converters, and thermal management of IGBT power modules in electrical drive applications.

R. RAJA SINGH (Member, IEEE) received the B.Tech. degree in electrical and electronics engineering from Pondicherry University, India, in 2004, the M.E. degree in power electronics and drives from Anna University, India, in 2008, and the Ph.D. degree in electrical drive systems from Indian Institute of Technology (IIT) Roorkee, India, in 2017. He is currently working as a Professor at the Automotive Research Center, Vellore Institute of Technology (VIT), Vellore, India. He has more than 15 years of teaching experience in India and Tanzania, as well as, five years of research experience at IIT Roorkee. He has developed various energy-efficient control strategies for industrial drives. He has four patents granted in the field of electrical drive systems. He has published more than 100 research papers in various journals and conferences of international repute. His research interests include power converters for renewable energy and Industrial applications, power quality control, starting transient and fault analysis on electric drives, electrical vehicle systems, and the IoT smart monitoring systems.